



**Effects of Genetic Perturbation on Seasonal Life
History Plasticity**

Amity M. Wilczek, *et al.*
Science **323**, 930 (2009);
DOI: 10.1126/science.1165826

**The following resources related to this article are available online at
www.sciencemag.org (this information is current as of February 14, 2009):**

Updated information and services, including high-resolution figures, can be found in the online version of this article at:

<http://www.sciencemag.org/cgi/content/full/323/5916/930>

Supporting Online Material can be found at:

<http://www.sciencemag.org/cgi/content/full/1165826/DC1>

This article **cites 26 articles**, 12 of which can be accessed for free:

<http://www.sciencemag.org/cgi/content/full/323/5916/930#otherarticles>

This article appears in the following **subject collections**:

Evolution

<http://www.sciencemag.org/cgi/collection/evolution>

Information about obtaining **reprints** of this article or about obtaining **permission to reproduce this article** in whole or in part can be found at:

<http://www.sciencemag.org/about/permissions.dtl>

of genes present in *Cotesia congregata* could constitute the remnants of the genome of this ancestral virus. The level of similarity between *HZNvorf9-like1* and *HZNvorf128-like* products from *Chelonus inanitus* and *Cotesia congregata* reaches 80% and thus indicates a strong conservation of their functions (Table 1). Some proteins show a lower conservation (for example for p74, 46% similarity), which suggests these sequences may be involved in more specific interactions with the host and have had to evolve more rapidly due to selective pressures associated with infection.

The overall conservation of the nudiviral machinery encoded by the wasps contrasts sharply with the lack of similarity found between the DNA enclosed in CiBV and CcBV particles. No common genes were found between CiBV and other bracovirus genomes (27); only sequences involved in the production of the circular dsDNAs of the particles (excision sequences) were conserved (28, 29). Furthermore, packaged bracovirus genomes do not contain any nudivirus-related genes. We hypothesize that shortly after initial integration of the nudivirus ancestor, viral DNA might have been replaced by wasp DNA in the particles (possibly by translocation of sequences allowing excision and encapsidation) and that most genes promoting parasitism were acquired later and independently in bracovirus-associated wasps.

It is well documented that genes of viral origin are used by eukaryotes to ensure physiological functions, such as the syncytins involved in trophoblast differentiation, which originated

from retroviral envelope proteins independently acquired by primates and mice (30). However, the bracovirus-wasp associations represent the only example, so far, of the incorporation of genes encoding a complex viral machinery that allows its eukaryotic host to transfer and express heterologous genes in target organisms. In this regard, unraveling bracovirus particle assembly could contribute to the design of new vectors for gene therapy.

References and Notes

- N. A. Moran, *Proc. Natl. Acad. Sci. U.S.A.* **104**, 8627 (2007).
- B. A. Webb, M. R. Strand, in *Comprehensive Molecular Insect Science*, L. I. Gilbert, K. Iatrou, S. S. Gill, Eds. (Elsevier, Amsterdam, 2005), vol. 6, pp. 323–360.
- S. Wyder, F. Blank, B. Lanzrein, *J. Insect Physiol.* **49**, 491 (2003).
- E. Espagne *et al.*, *Science* **306**, 286 (2004).
- J. A. Kroemer, B. A. Webb, *Annu. Rev. Entomol.* **49**, 431 (2004).
- J. B. Whitfield, S. Asgari, *J. Insect Physiol.* **49**, 397 (2003).
- B. A. Federici, Y. Bigot, *J. Insect Physiol.* **49**, 419 (2003).
- J. B. Whitfield, *Proc. Natl. Acad. Sci. U.S.A.* **99**, 7508 (2002).
- H. Thoeftkiattikul, M. H. Beck, M. R. Strand, *Proc. Natl. Acad. Sci. U.S.A.* **102**, 11426 (2005).
- B. Provost *et al.*, *J. Virol.* **78**, 13090 (2004).
- E. Espagne *et al.*, *J. Virol.* **79**, 9765 (2005).
- L. Deng, D. B. Stoltz, B. A. Webb, *Virology* **269**, 440 (2000).
- Materials and methods are available as supporting material on Science Online.
- A. M. Abd-Alla *et al.*, *J. Virol.* **82**, 4595 (2008).
- Y. Wang, R. G. Kleespies, A. M. Huger, J. A. Jehle, *J. Virol.* **81**, 5395 (2007).
- E. A. Herniou, J. A. Olszewski, J. S. Cory, D. R. O'Reilly, *Annu. Rev. Entomol.* **48**, 211 (2003).
- A. L. Vanarsdall, V. S. Mikhailov, G. F. Rohrmann, *Curr. Drug Targets* **8**, 1096 (2007).

- M. M. van Oers, J. M. Vlask, *Curr. Drug Targets* **8**, 1051 (2007).
- A. L. Passarelli, L. A. Guarino, *Curr. Drug Targets* **8**, 1103 (2007).
- S. C. Braunagel, M. D. Summers, *Curr. Drug Targets* **8**, 1084 (2007).
- R. R. Granados, T. Nguyen, B. Cato, *Intervirology* **10**, 309 (1978).
- A. K. Raina *et al.*, *J. Invertebr. Pathol.* **76**, 6 (2000).
- C. H. Cheng *et al.*, *J. Virol.* **76**, 9024 (2002).
- Y. Wang, R. G. Kleespies, M. B. Ramlé, J. A. Jehle, *J. Virol. Methods* **152**, 106 (2008).
- N. Murphy, J. C. Banks, J. B. Whitfield, A. D. Austin, *Mol. Phylogenet. Evol.* **47**, 378 (2008).
- F. Pasquier-Barre *et al.*, *J. Gen. Virol.* **83**, 2035 (2002).
- B. Weber, M. Annaheim, B. Lanzrein, *Arch. Insect Biochem. Physiol.* **66**, 9 (2007).
- M. Annaheim, B. Lanzrein, *J. Gen. Virol.* **88**, 450 (2007).
- C. A. Desjardins *et al.*, *BMC Microbiol.* **7**, 61 (2007).
- F. Mallet *et al.*, *Proc. Natl. Acad. Sci. U.S.A.* **101**, 1731 (2004).
- Investigations of *C. congregata* and *H. didymator* were performed as part of the project EVPARASITOID supported by the agencies Agence Nationale de la Recherche (France) and CNRS (GDR 2153, GDR 2157, and IFR 136). *C. inanitus* study was supported by the Swiss National Science Foundation (grants 3100A0-103964 and 116067 to B.L.). We thank E. Herniou for helpful discussions and C. Ménoiret and C. Labrousse for insect-rearing. Sequences have been deposited in the EMBL Nucleotide Sequence Database, accession numbers FM201559-80, FM201582-97, and FM877774 for the viral cDNAs and FM212911-15 for the chromosomally integrated form of nudivirus-related genes.

Supporting Online Material

www.sciencemag.org/cgi/content/full/323/5916/926/DC1

Material and Methods

Fig. S1

Tables S1 to S5

References

3 October 2008; accepted 18 December 2008

10.1126/science.1166788

Effects of Genetic Perturbation on Seasonal Life History Plasticity

Amity M. Wilczek,¹ Judith L. Roe,² Mary C. Knapp,² Martha D. Cooper,¹ Cristina Lopez-Gallego,^{1*} Laura J. Martin,^{1†} Christopher D. Muir,^{1‡} Sheina Sim,^{2§} Alexis Walker,¹ Jillian Anderson,¹ J. Franklin Egan,^{1||} Brook T. Moyers,^{1¶} Renee Petipas,^{1#} Antonis Giakountis,³ Erika Charbit,² George Coupland,³ Stephen M. Welch,² Johanna Schmitt^{1**}

Like many species, the model plant *Arabidopsis thaliana* exhibits multiple different life histories in natural environments. We grew mutants impaired in different signaling pathways in field experiments across the species' native European range in order to dissect the mechanisms underlying this variation. Unexpectedly, mutational loss at loci implicated in the cold requirement for flowering had little effect on life history except in late-summer cohorts. A genetically informed photothermal model of progression toward flowering explained most of the observed variation and predicted an abrupt transition from autumn flowering to spring flowering in late-summer germinants. Environmental signals control the timing of this transition, creating a critical window of acute sensitivity to genetic and climatic change that may be common for seasonally regulated life history traits.

The seasonal timing of critical life history events is often under strong natural selection, requiring plants to integrate and respond appropriately to multiple environmental signals. In the case of flowering time, these in-

clude day length, ambient temperature, and winter chilling (vernalization) cues. Genetic mechanisms of flowering response to environmental cues have been well characterized in the model plant *Arabidopsis thaliana* in the laboratory. However,

the response of *Arabidopsis* to complex, natural environmental cues is unknown. The native distribution of *Arabidopsis* encompasses climates from the Mediterranean, where it is a winter annual that germinates in late autumn and flowers in late winter or early spring, to northern Scandinavia, where the species germinates in early autumn, overwinters, and flowers in late spring and early summer. In England and northwestern Europe, *Arabidopsis* either is a winter annual or undergoes rapid cycling by germinating in early autumn, spring, or summer, thus flowering without vernalization (1, 2). Thus, in nature the species experiences marked variation in photothermal environments across sites and seasons.

The timing and environmental sensitivity of flowering in *Arabidopsis* are regulated by a network of genes in several converging pathways (3–5) (fig. S1). Inductive long days are perceived by the photoperiod pathway, which accelerates flowering acting through *GIGANTEA* (*GI*) and *CONSTANS* (*CO*) (6, 7). The gibberellin pathway (8) and high temperatures (9–12) also promote flowering. These signals activate floral integrator genes such as *FLOWERING LOCUS T* (*FT*) (3). The ability of these integrators to respond is controlled by repressor genes, notably *FLOWERING*

LOCUS C (FLC), which in turn is activated by genes such as *FRIGIDA (FRI)* and is repressed by vernalization and by genes in the autonomous pathway such as *LUMINIDEPENDENS (LD)* and *FVE (13)*. Prolonged exposure to cold induces *VERNALIZATION-INSENSITIVE-3 (VIN3)*, which initiates stable epigenetic repression of *FLC (13–15)*. Deficiencies in *FLC* activators such as *FRI* remove the vernalization requirement for flowering and may cause a rapid-cycling life history (16, 17).

To assess the relative contributions of different signaling pathways across environments, we grew mutants impaired in response to specific environmental signals and documented environmental conditions at five field sites spanning the native European climatic range: Oulu, Finland; Norwich, UK; Cologne and Halle, Germany; and Valencia, Spain (figs. S2 and S3) (18). Across these sites, we established a total of nine seasonal cohorts timed to coincide with the germination of local natural populations (fig. S2). To compare the relative contribution of the photoperiod pathway to flowering across sites and seasons, we examined the flowering delay in mutants of *CO*, which is activated by long-day signals, and in mutants of *GI*, which promotes flowering both by activating *CO (19)* and through a *CO*-independent derepression of *FT (20)*. Both photoperiod pathway mutants (*co-2* in Ler, *gi-2* in Col) showed initiation of flowering significantly later than in the wild type in all plantings except for those planted at Halle in the fall (Fig. 1 and table S1). These mutants flowered especially late in the summer plantings and the Norwich fall cohort, planted under declining long days (Fig. 1).

To examine the effects of different *FLC* repression levels, and thus vernalization requirements, we compared the *fri* null Col-0 wild-type to Col-*FRI-Sf2*, which contains an introgressed strong allele of the *FLC* activator *FRI* that naturally occurs in the *Sf-2* ecotype (21). We also examined the effects of the autonomous pathway mutants *ld-1*, *fve-3*, and *fve-4*, which impair repression of *FLC* expression and delay flow-

ering in the absence of vernalization, even in a null *fri* background (22). Col-*FRI-Sf2* and the autonomous pathway mutants flowered at similar times within each of the plantings. Although *FRI* introgression and autonomous pathway mutation were expected to confer constitutive winter-annual life histories on the basis of greenhouse studies (6, 21), these lines displayed delays of only ~10 days when planted in summer cohorts, which lacked vernalization (table S2). Thus, *FLC*-induced repression of flowering can be overridden, possibly as a result of natural temperature fluctuations (fig. S4) (23) or light conditions (21). Col-*FRI-Sf2* and the autonomous pathway mutants both demonstrated small but significant delays in bolting in the spring cohorts and displayed an expected winter-annual life history in all autumn plantings (Fig. 1 and table S1). However, the Col wild type behaved as a rapid cyclers (its laboratory phenotype) only in Norwich, where it flowered in fall more than 100 days earlier than did Col-*FRI-Sf2* and Col plants containing autonomous pathway mutations. Unexpectedly, in the remaining autumn cohorts, Col flowered much later than in Norwich, displaying a clear winter-annual life history in Halle. Thus, loss of *FRI* function converts winter annuals to rapid cyclers only under a narrow range of natural environmental conditions.

The *vin3-1* deletion, which is deficient in its ability to respond to vernalization cues, had no significant effect on flowering time in the summer cohorts relative to the vernalization-sensitive background wild type (Col-*FRI-Sf2*) (Fig. 1 and table

S1), as expected. In contrast, *vin3-1* mutants flowered later than the control in autumn plantings in a manner that was correlated with exposure to vernalizing temperatures (fig. S3C). Additionally, *vin3-1* mutation significantly delayed flowering in spring cohorts (Fig. 1), where plants were exposed to vernalizing temperatures early in development (fig. S3C). Thus, vernalization signals predominated in the later autumn cohorts, photoperiod predominated in summer plantings, and both substantially contributed to the flowering response of spring-germinating plants.

We created a genetically informed photothermal model of *Arabidopsis* development in which plants transition from nonflowering rosettes to bolting (the first visible sign of floral initiation) once they have accumulated a threshold number of environmentally determined photothermal developmental units—temporal measures that incorporate climatic conditions and are interchangeable with real time [e.g., (24)]. Phenology models empirically scale photothermal units so that developmental transitions occur at a common threshold of accumulated units independent of particular environmental conditions. The accumulation of appropriately scaled photothermal units over time will therefore show the developmental progression of plants toward the initiation of reproductive growth (Fig. 2). We extended classical phenological modeling approaches by linking individual scaling factors to the activities of specific genes and their regulators. In our gene network-based model, each genotype accumu-

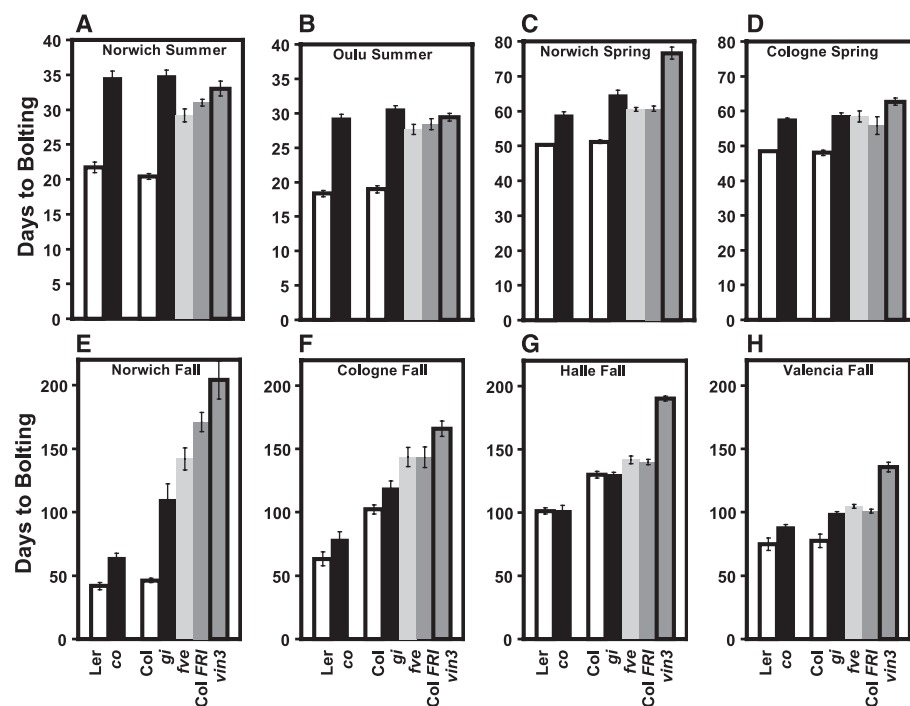


Fig. 1. Sensitivity of flowering-time pathways across sites and seasons. Bars show mean bolting times (\pm SE) of mutants in different flowering-time pathways along with their wild-type controls. (A) Norwich summer 2007 planting; (B) Oulu summer 2006; (C) Norwich spring 2007; (D) Cologne spring 2007; (E) Norwich fall 2006; (F) Cologne fall 2006; (G) Halle fall 2006; (H) Valencia fall 2006. Note the difference in scale among locations and seasons.

¹Department of Ecology and Evolutionary Biology, Brown University, Providence, RI 02912, USA.

²Department of Agronomy, Kansas State University, Manhattan, KS 66506, USA.

³Max Planck Institute for Plant Breeding Research, Cologne D-50829, Germany.

*Present address: Biology Institute, Universidad de Antioquia, Medellin AA 1226, Colombia.

†Present address: Department of Natural Resources, Cornell University, Ithaca, NY 14853, USA.

‡Present address: Department of Biology, Indiana University, Bloomington, IN 47405, USA.

§Present address: Department of Biological Sciences, University of Notre Dame, Notre Dame, IN 46556, USA.

||Present address: Department of Crop and Soil Sciences, Pennsylvania State University, University Park, PA 16802, USA.

¶Present address: Department of Botany, University of British Columbia, Vancouver, BC V6T 1Z4, Canada.

#Present address: Department of Biology, University of Vermont, Burlington, VT 05405, USA.

**To whom correspondence should be addressed. E-mail: johanna_schmitt@brown.edu

Fig. 2. The accumulation of modified photothermal units from the time of sowing for genotypes in the Col background differing in environmental sensitivity. The model estimated the threshold for bolting at 2604 modified photothermal units (horizontal dashed line), a constant for all environments and genotypes. Each genotype is depicted by a single trace, which shows the accumulation of modified photothermal units in that particular mutant or wild-type background. Observed bolting times (days on the x axis, modified photothermal units on the y axis) with confidence intervals are shown on each of the accumulation traces. Note differences in scale of x axis among seasons. (A) Norwich summer 2007; (B) Norwich spring 2007; (C) Norwich fall 2006; (D) Halle fall 2006.

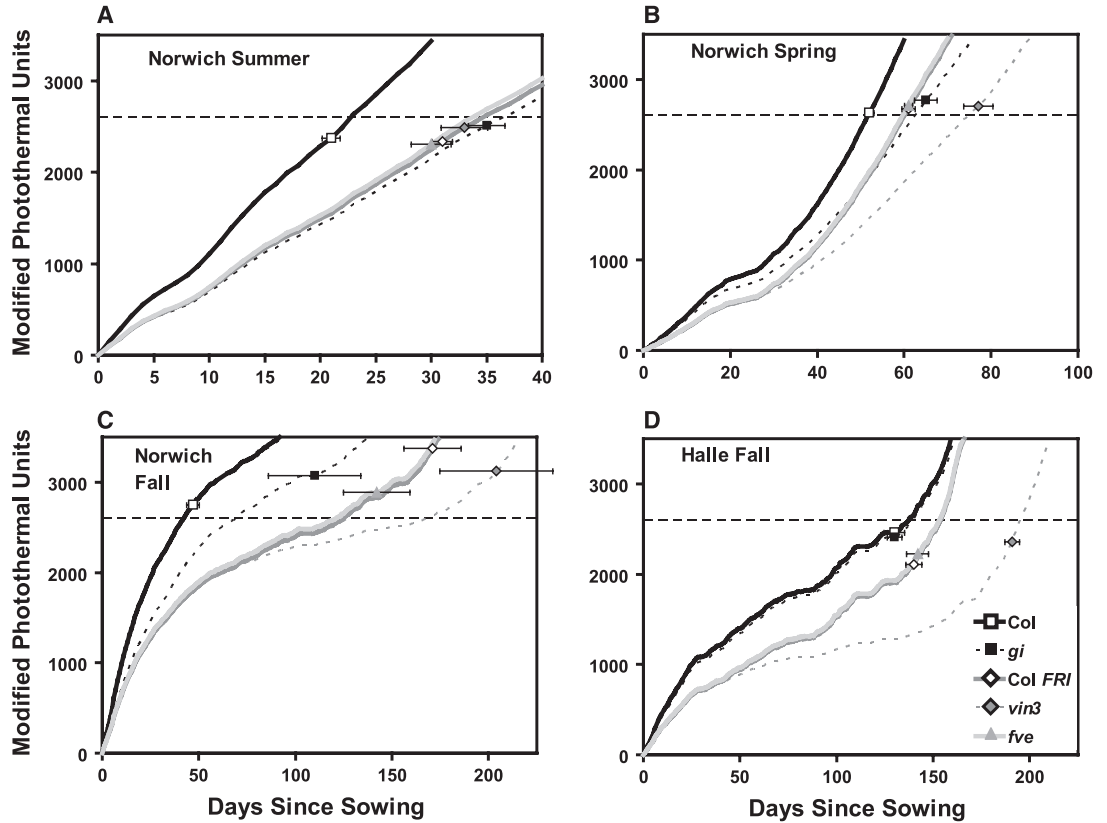
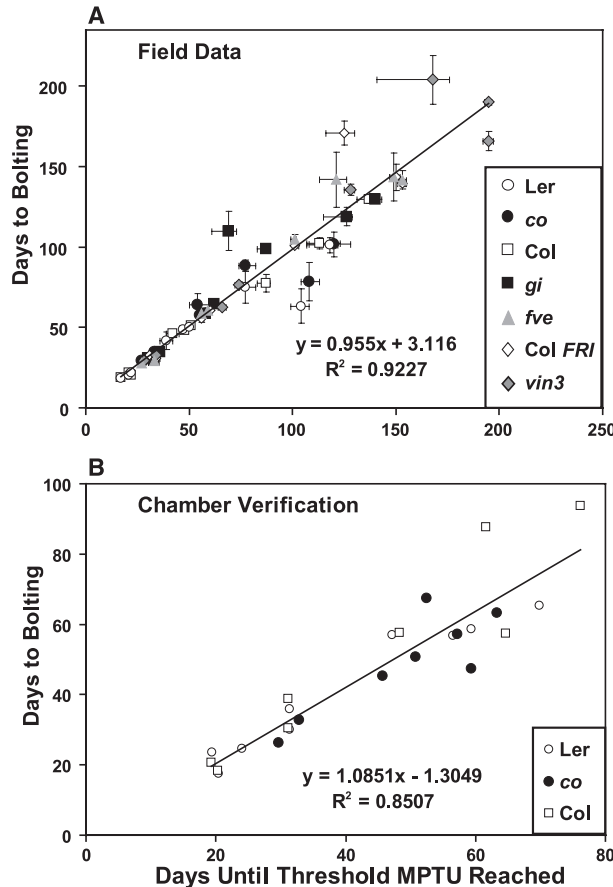


Fig. 3. Observed versus predicted bolting times. (A) Field-observed bolting phenotypes of Ler-1, *co-2*, Col-0, *gi-2*, Col-*FRI-Sf2*, *vin3-1* (in Col-*FRI-Sf2*), and *fve-3* across the nine experimental plantings and the predicted phenotypes from the fitted model. Line means with confidence intervals are shown. Confidence intervals for the modified photothermal units (MPTU) were back-calculated to find the day at which the lower and upper 95% confidence limit for the bolting threshold was reached. (B) Verification against growth chamber data not used in model construction, showing results from Ler, *co* (both *co-2* and *co-3*), and Col across nine treatments in two experiments.



lated photothermal units on the basis of day lengths and hourly temperature averages in each experimental planting, modified according to the environmental sensitivity of the line. For example, in our model, both photoperiod mutants and wild-type lines (Col versus *gi-2*, Ler versus *co-2*) were assumed to develop at similar rates under short days.

Photoperiod mutants did not respond to increasing day length, but the modeled developmental rate of wild-type plants accelerated above a critical short day length (Fig. 2) until a maximum rate was reached at a saturating long day length (25). Chamber experiments confirmed this piecewise linear response to day length in the Ler accession and identified a critical short day length of ~10 hours. However, flowering in the *co-2* mutant was insensitive to day length (fig. S5). Development was also assumed to accelerate during vernalization because of the repression of *FLC*, with the modeled degree of acceleration varying according to genetic background (Ler versus Col), the allelic state of *FRI* (Col *fri* versus Col *FRI*), and the presence or absence of functional alleles in the autonomous pathway (Col versus *ld* and *fve*); however, *vin3-1* plants did not experience any *FLC* repression from exposure to cold temperatures (Fig. 2). A novel feature of the model, resulting from the scaling of developmental rate with pathway activities, was that all mutants within a given genetic background were predicted to flower at a common threshold of modified photothermal units. Parameter values for the critical day length window, vernalization effective-

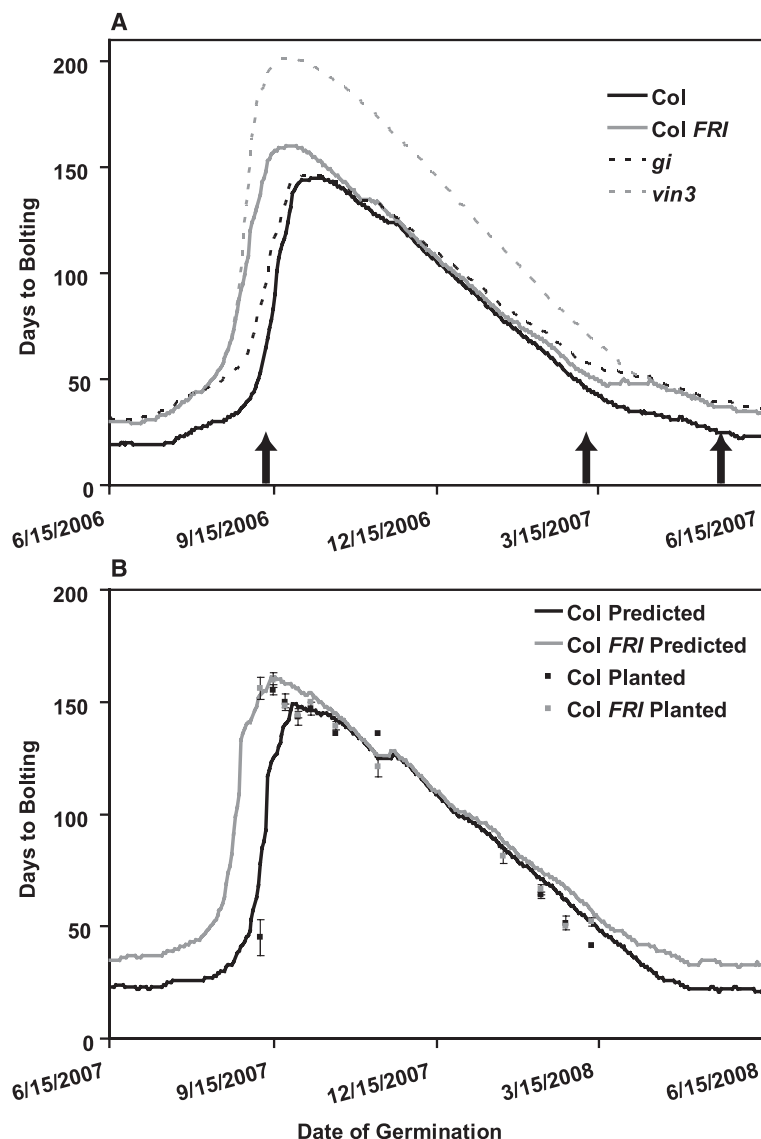


Fig. 4. Timing of bolting as a function of time of germination. **(A)** In Norwich, a narrow window of extreme sensitivity to germination timing is predicted when sown in early autumn. Timing of experimental sowings is shown by arrows. **(B)** Model validation in Cologne with measured bolting data from repeated plantings of *FRI* functional and nonfunctional ecotypes into the field from September 2007 through March 2008. Our model predicted 94% of the variation in bolting time, confirming the expectation that *FRI* results in a life history conversion in early-autumn cohorts.

ness temperature function, time until vernalization saturation, and the degree-hour base temperature were drawn from empirical studies (table S3). Short-day developmental rate and the initial levels of *FLC* repression of development were optimized to the lowest coefficient of variation of modified photothermal units accumulated at observed bolting times across all plantings (18).

Our best-fit model explained more than 92% of the observed overall variance in days to bolting (Fig. 3A) and was in agreement with observed reversals in flowering-time order of different genotypes across plantings (e.g., *gi-2* versus Col-*FRI-Sf2*, Cologne and Norwich spring versus fall; Fig. 2 and table S2). The model, with parameter values derived from our field experi-

ment, also accurately predicted the behavior of plants not used in the model's construction and accounted for most of the flowering-time variation of Col, Ler, and *co* mutants under a wide range of controlled conditions [(11) and table S4; $R^2 = 0.85$ for the data in both studies, Fig. 3B]. Thus, a modified photothermal model, informed by understanding of pathway function and empirical measurements of gene effects in controlled environments, can be used to quantify the shifting balance and sensitivity of flowering-time pathways under a broad range of climate conditions.

We examined the relative sensitivity of flowering time to parameters representing vernalization sensing, day length sensing, short-day development rate, and baseline *FLC* levels (table S3)

and found that flowering time was most sensitive to the initial *FLC* level in both Col and Ler. The short-day development rate, which represents the baseline at which plants proceed toward flowering in the absence of long-day or vernalization cues, had a large effect on flowering time. Indeed, development was slowed by 60 to 74% before vernalization depending on background, and short-day development proceeded only 63 to 69% as quickly as in long days. Similar genetically based sensitivity to photoperiod and/or vernalization cues has been observed in other species and traits (24, 26), in some cases with similar integration of converging pathways (27–29). The linking of scaling factors to pathway activity depends on network architecture rather than gene identity, which suggests that similar models will prove useful in other species, even where the genes involved do not share a common evolutionary history.

Our model also was able to predict the effects of novel environments on flowering time across genotypes. For example, we used the model to generate predicted reaction norms of flowering date to germination timing in Norwich and Cologne, using actual daily on-site photothermal data to simulate the flowering dates of seeds germinating on successive days over a yearly cycle (Fig. 4). The model predicted a striking, abrupt transition from rapid-cycling to winter-annual life histories for all genotypes germinating in late summer. During this narrow temporal window of sensitivity, all genotypes switched from autumn to spring flowering; the high-*FLC* lines Col-*FRI-Sf2* and *vin3-1* transitioned between life histories earliest and showed the largest flowering-time response (Fig. 4). A series of repeated plantings into the field in Cologne of Col and Col-*FRI-Sf2* seedlings throughout the autumn and spring confirmed the predicted abrupt life history transition (Fig. 4B, $R^2 = 0.94$). This rapid rise in bolting time with later germination in autumn will be general across many climates, as it is driven by common patterns of seasonal periodicity of light and temperature cues (fig. S6). Thus, the impact of genetic perturbation on flowering time and life history expression under natural conditions is acutely sensitive to germination timing.

Our results suggest that *A. thaliana* ecotypes cannot simply be divided into two discrete classes of winter-annual and rapid-cycling genotypes. Rather, most ecotypes may be capable of both life histories but vary in the sensitivity and timing of the rapid transition between them. Consequently, natural variation in flowering pathways may have the greatest phenotypic expression and exposure to natural selection in climates that permit late-summer germination. Although the current model was developed for *A. thaliana*, the underlying principle of linking genetic architecture to environmental sensitivity is broadly applicable across plant species and seasonal traits. Our ability to predict the consequences of genetic variation under current and future climates has

implications for optimizing plant breeding and cultivation strategies.

References and Notes

1. F. Laibach, *Arabidopsis Information Service 015* (1965).
2. L. Thompson, *J. Ecol.* **82**, 63 (1994).
3. Y. Kobayashi, D. Weigel, *Genes Dev.* **21**, 2371 (2007).
4. I. Ausin, C. Alonso-Blanco, J. M. Martinez-Zapater, *Int. J. Dev. Biol.* **49**, 689 (2005).
5. I. Baurle, C. Dean, *Cell* **125**, 655 (2006).
6. M. Koornneef, C. J. Hanhart, J. H. van der Veen, *Mol. Gen. Genet.* **229**, 57 (1991).
7. J. Putterill, F. Robson, K. Lee, R. Simon, G. Coupland, *Cell* **80**, 847 (1995).
8. R. N. Wilson, J. W. Heckman, C. R. Somerville, *Plant Physiol.* **100**, 403 (1992).
9. M. A. Blazquez, J. H. Ahn, D. Weigel, *Nat. Genet.* **33**, 168 (2003).
10. S. M. Welch, J. L. Roe, Z. Dong, *Agron. J.* **95**, 71 (2003).
11. J. Lempe *et al.*, *PLoS Genet.* **1**, e6 (2005).
12. S. Balasubramanian, S. Sureshkumar, J. Lempe, D. Weigel, *PLoS Genet.* **2**, e106 (2006).
13. R. J. Schmitz, R. M. Amasino, *Biochim. Biophys. Acta* **1769**, 269 (2007).
14. S. Sung, R. M. Amasino, *Nature* **427**, 159 (2004).
15. E. S. Dennis, W. J. Peacock, *Curr. Opin. Plant Biol.* **10**, 520 (2007).
16. G. G. Simpson, C. Dean, *Science* **296**, 285 (2002).
17. S. D. Michaels, Y. H. He, K. C. Scortecchi, R. M. Amasino, *Proc. Natl. Acad. Sci. U.S.A.* **100**, 10102 (2003).
18. See supporting material on Science Online.
19. T. Mizoguchi *et al.*, *Plant Cell* **17**, 2255 (2005).
20. J. H. Jung *et al.*, *Plant Cell* **19**, 2736 (2007).
21. I. Lee, R. M. Amasino, *Plant Physiol.* **108**, 157 (1995).
22. S. D. Michaels, R. M. Amasino, *Plant Cell* **13**, 935 (2001).
23. L. T. Burghardt *et al.*, in *19th International Conference on Arabidopsis Research* (Montreal, 23–27 July 2008), abstract ICAR802.
24. G. S. McMaster *et al.*, *Ann. Bot.* **102**, 561 (2008).
25. S. M. Welch, Z. Dong, J. L. Roe, *Aust. J. Agric. Res.* **56**, 919 (2005).
26. J. P. De Melo-Abreu *et al.*, *Agric. For. Meteorol.* **125**, 117 (2004).
27. G. T. Howe *et al.*, *Can. J. Bot.* **81**, 1247 (2003).
28. H. Böhlenius *et al.*, *Science* **312**, 1040 (2006); published online 3 May 2006 (10.1126/science.1126038).
29. J. Cockram *et al.*, *J. Exp. Bot.* **58**, 1231 (2007).
30. We thank M. Blazquez, C. Dean, M. Hoffmann, M. Koornneef, H. Kuittinen, and O. Savolainen for hosting these experiments at the European field sites; L. Albertson, L. Burghardt, C. Cooper, M. F. Cooper, E. Josephs, A. Lockwood, S. Myllylä, C. Oakley, R. Palmer, S. Rudder, and E. vonWettberg for assistance with planting and censusing; B. Robertson, M. Gosling, C. Lister, F. Eikelmann, G. Leuffen, W. Schuchert, T. Kauppila, and H. Eissner for technical and field assistance; R. Griffin, J. Kreikemeier, and G. Ragusa for assistance with the chamber experiment; A. Heim for contributions to the processing of temperature data; R. Amasino and J. Martinez-Zapater for sharing lines; S. Ruzsa of the Puruggan lab, who bulked lines for the experiments; and R. Amasino and C. Dean for manuscript comments. Supported by NSF Frontiers in Integrative Biological Research program grant EF-0425759 and an Alexander von Humboldt Research Award.

Supporting Online Material

www.sciencemag.org/cgi/content/full/1165826/DC1
Materials and Methods
Figs. S1 to S11
Tables S1 to S6
References

11 September 2008; accepted 19 November 2008
Published online 15 January 2009;
10.1126/science.1165826
Include this information when citing this paper.

The Hallucinogen *N,N*-Dimethyltryptamine (DMT) Is an Endogenous Sigma-1 Receptor Regulator

Dominique Fontanilla,¹ Molly Johannessen,² Abdol R. Hajjipour,³ Nicholas V. Cozzi,¹ Meyer B. Jackson,² Arnold E. Ruoho^{1*}

The sigma-1 receptor is widely distributed in the central nervous system and periphery. Originally mischaracterized as an opioid receptor, the sigma-1 receptor binds a vast number of synthetic compounds but does not bind opioid peptides; it is currently considered an orphan receptor. The sigma-1 receptor pharmacophore includes an alkylamine core, also found in the endogenous compound *N,N*-dimethyltryptamine (DMT). DMT acts as a hallucinogen, but its receptor target has been unclear. DMT bound to sigma-1 receptors and inhibited voltage-gated sodium ion (Na⁺) channels in both native cardiac myocytes and heterologous cells that express sigma-1 receptors. DMT induced hypermobility in wild-type mice but not in sigma-1 receptor knockout mice. These biochemical, physiological, and behavioral experiments indicate that DMT is an endogenous agonist for the sigma-1 receptor.

The sigma-1 receptor binds a broad range of synthetic compounds (1). It has long been suspected that the sigma-1 receptor is targeted by endogenous ligands, and several candidates have been proposed (2, 3). Although progesterone and other neuroactive steroids are known to bind sigma-1 receptors and regulate some of their functions (1, 4), they do not exhibit agonist properties on sigma-1-regulated ion channels in electrophysiological experiments (5).

Our search for a sigma receptor endogenous ligand (or ligands) was based on a variant of the

canonical sigma-1 receptor ligand pharmacophore (6), but with a more basic structure (Fig. 1A). Otherwise dissimilar sigma-1 receptor ligands possess a common *N*-substituted pharmacophore (Fig. 1A): an *N,N*-dialkyl or *N*-alkyl-*N*-aralkyl product, most easily recognized in the high-affinity sigma-1 receptor ligand, fenpropimorph (7). Similar chemical backbones can be derived from other sigma-1 receptor ligands such as haloperidol and cocaine (Fig. 1A). *N*-substituted trace amines harbor this sigma-1 receptor ligand pharmacophore, but their interactions with sigma receptors have not been determined. Of particular interest is the only known endogenous mammalian *N,N*-dimethylated trace amine, *N,N*-dimethyltryptamine (DMT) (8–10). In addition to being one of the active compounds in psychoactive snuffs (*yopo*, *ependá*) and sacramental teas (*ayahuasca*, *yagé*) used in native shamanic rituals in South America, DMT can be produced by enzymes in mammalian lung (11) and in rodent

brain (12). DMT has been found in human urine, blood, and cerebrospinal fluid (9, 13). Although there are no conclusive quantitative studies measuring the abundance of endogenous DMT because of its rapid metabolism (14), DMT concentrations can be localized and elevated in certain instances. Evidence suggests that DMT can be locally sequestered into brain neurotransmitter storage vesicles and that DMT production increases in rodent brain under environmental stress (8). Although a family of heterotrimeric GTP-binding protein (G protein)-coupled receptors (GPCRs) known as the trace amine receptors (TARs) was discovered in 2001 (15), only two members of this family respond to trace amines and have been renamed trace amine-associated receptors (TAARs) (16). Because other binding targets for trace amines and DMT are likely (8), we first examined the sigma-1 receptor binding affinities of the trace amines and their *N*-methylated and *N,N*-dimethylated counterparts.

Competition assays against the sigma-1 receptor-specific ligand, (+)-[³H]-pentazocine (10 nM), determined that the nonmethylated trace amines tryptamine, phenethylamine, and tyramine bound the sigma-1 receptor poorly (Fig. 1C), with dissociation constant (K_d) values of 431, 97.4, and >30,000 μ M, respectively. By contrast, the *N*-methylated and *N,N*-dimethylated derivatives of these compounds bound sigma-1 receptors more tightly, with a clear increase in affinity as the ligands approached the sigma-1 receptor ligand and pharmacophore (Fig. 1, A and B). With the exception of the *N*-methylated tyramines, this trend did not apply to the sigma-2 receptor, which differs pharmacologically and functionally from the sigma-1 receptor (Fig. 1C). Tryptamine, phenethylamine, and *N*-methyltryptamine had the highest sigma-2 receptor affinities, with K_d values of 4.91, 7.31, and 6.61 μ M, respectively. In contrast to sigma-1 receptors, *N*-methylation and *N,N*-

¹Department of Pharmacology, University of Wisconsin School of Medicine and Public Health, Madison, WI 53706, USA.

²Department of Physiology, University of Wisconsin School of Medicine and Public Health, Madison, WI 53706, USA.

³Pharmaceutical Research Laboratory, Department of Chemistry, Isfahan University of Technology, Isfahan 84156, IR Iran.

*To whom correspondence should be addressed. E-mail: aeruoho@wisc.edu